Materials Research Proceedings **27** (2023) 259-264 https://doi.org/10.21741/9781644902455-33

Higher-order effects of amplitude-modulation vibro-acoustic technique for characterization thermal damages in cement-based material

Tingyuan Yin[1, a *], Ching Tai Ng[1,b] and Andrei Kotousov[2,c]

[1]School of Civil, Environmental and Mining Engineering, The University of Adelaide, SA 5005, Australia

[2]School of Mechanical Engineering, The University of Adelaide, SA 5005, Australia

[a]tingyuan.yin@adelaide.edu.au, [b]alex.ng@adelaide.edu.au, [c]andrei.kotousov@adelaide.edu.au

Keywords: Third-Order, Elastic Constant, Amplitude-Modulation, Vibro-Acoustic Technique, Thermal Damages, Cement-Based Material

Abstract. This paper proposes a new amplitude-modulation vibro-acoustic (AMVA) technique to detect thermal damage in pristine graphene (PRG) mortar materials. A new third-order solution for an amplitude-modulated low-frequency pump wave and a high-frequency probe wave in infinite isotropic material is presented. The solution includes higher-order sidebands generated by intrinsic and acquired nonlinearities. A nonlinear parameter is defined according to the third-order solution to assess the different levels of thermal damage. The experimental study demonstrates the sensitivity and feasibility of the AMVA technique by comparing the nonlinear parameter with the linear measurements of the ultrasonic pulse velocity (UPV) test. The results show that the proposed AMVA technique is a potential tool to detect and monitor thermal damage in cement-based structures.

Introduction

The exceptional durability and excellent mechanical properties of cement-based material are the primary reasons cement-based material is one of the most popular construction materials worldwide. However, material limitations, design and construction practices, and severe exposure conditions can cause cement-based material to deteriorate, which leads to aesthetic, functional, or safety problems [1-3]. Therefore, there is a powerful incentive to develop nondestructive testing (NDT) techniques for damage detection and structural health monitoring (SHM) techniques for long-term in-situ monitoring of structures.

The vibro-acoustic technique is one of the promising techniques for damage detection in cement-based material since the low-frequency (LF) pump wave can provide an intensive field to perturb the defects and cracks while the high-frequency (HF) probe wave is sensitive to microscale damages because of its small wavelength [4-7]. The interaction of the pump wave and probe wave in the nonlinear system, which contains distributed nonlinearity or localized nonlinearity, reveals as sidebands in the frequency spectrum. Assuming the frequency of LF pump wave is f_L, while HF probe wave is f_H, thus it can be found that the sidebands show at the frequency of $f_H \pm N \cdot f_L$ $(N = 1,2,3 \dots)$. The index for damage evaluation is generally related to the sidebands and fundamental components. Furthermore, the measurements of the vibro-acoustic technique are less affected by unwanted nonlinear sources, such as the data acquisition system and coupling conditions. The combination of the LF pump wave and the HF probe wave brings benefits to damage detection, but it also has some deficiencies in applications. First, the selection of frequency of LF pump wave is a key procedure. When choosing a higher LF pump wave, the frequency range of sidebands $f_H \pm N \cdot f_L$ is broad, and hence, a broadband receiving instrument is needed, such as a laser vibrometer or broadband transducer which is usually costly. While using a lower LF pump

wave will result in a large burden to the emitting instrument, such as an electro-forced shaker, particularly for a long-term monitoring. Therefore, studies have been carried out to develop a vibro-acoustic technique by i) enhancing the practical procedures, ii) inducing novel signal processing approaches, and iii) utilizing new pump and probe waves.

It is interesting that many studies have been conducted to apply pump and probe waves in vibro-acoustic techniques. Duffour P *et al.* carried out a study that a swept HF wave was applied, and LF excitation is the resonant response of the steel beam [8]. Frouin J *et al.* proposed a vibro-acoustic technique in which the LF pump wave was fixed while HF was swept wave in a broad range [9]. Dziedziech K *et al.* used swept waves for pump wave and probe wave [10]. Apart from the swept wave, Yin T *et al*. proposed three amplitude-modulated vibro-acoustic methods where LF pump wave was pre-amplitude-modulated to achieve lower energy consumption and versatility [11, 12]. However, in the previous study, the effect of higher-order sidebands sometimes was not considered, but it is sensitive to defects and cracks, resulting in increasing amplitude and numbers of sidebands. This study investigates the effect of higher-order sidebands in the amplitude-modulated vibro-acoustic technique. Meanwhile, a nonlinear parameter based on the higher-order sidebands is established for the characterization of thermal damage in cement-based material.

Theory

Considering the 1D elastodynamic wave equation written as,

$$\frac{\partial^2 u}{\partial t^2} = c^2[1 - \beta\frac{\partial u}{\partial x} - \gamma\left(\frac{\partial u}{\partial x}\right)^2]\frac{\partial^2 u}{\partial x^2}. \tag{1}$$

where u is the particle displacement, and the total solution $u = u_1 + u_2 + u_3$ is valid under the assumption $u_1 \gg u_2 \gg u_3$. In addition, t is the time, and x is the Lagrangian coordinate. β and γ are the nonlinear parameters. Hence, Eq.(1) can be decoupled into,

$$\frac{\partial^2 u_1}{\partial t^2} - c^2\frac{\partial^2 u_1}{\partial x^2} = 0. \tag{2}$$

$$\frac{\partial^2 u_2}{\partial t^2} + c^2\beta\frac{\partial u_1}{\partial x}\frac{\partial^2 u_1}{\partial x^2} - c^2\frac{\partial^2 u_2}{\partial x^2} = 0. \tag{3}$$

$$\frac{\partial^2 u_3}{\partial t^2} + c^2\gamma\left(\frac{\partial u_1}{\partial x}\right)^2\frac{\partial^2 u_1}{\partial x^2} + c^2\beta\frac{\partial u_2}{\partial x}\frac{\partial^2 u_1}{\partial x^2} + c^2\beta\frac{\partial u_1}{\partial x}\frac{\partial^2 u_2}{\partial x^2} - c^2\frac{\partial^2 u_3}{\partial x^2} = 0. \tag{4}$$

The input signal of AMVA technique is,

$$u_1 = A_H\cos(\omega_H\tau + \phi_H) + A_{L2}\cos(\omega_{L2}\tau + \phi_{L2})[1 + A_{L1}\cos(\omega_{L1}\tau + \phi_{L1})]. \tag{5}$$

where $A_H\cos(\omega_H\tau + \phi_H)$ is the HF probe wave, and the subscript H denotes the probe wave. Furthermore, $A_{L2}\cos(\omega_{L2}\tau + \phi_{L2})[1 + A_{L1}\cos(\omega_{L1}\tau + \phi_{L1})]$ is the amplitude-modulated LF pump wave.

Inserting Eq.(5) into Eq.(3), it can be found that the nonlinear parameter is related to sidebands as follow,

$$\beta^{(2)} \sim A_{(\omega_H \pm \omega_{L2})} \; and \; A_{(\omega_H \pm \omega_{L2} \pm \omega_{L2})}. \tag{6}$$

where the superscript (2) of β indicates the nonlinear parameter only considering the second displacement field u_2. Substituting the solution of u_1 and u_2 into Eq.(4), it can be seen that,

Materials Research Proceedings **27** (2023) 259-264 https://doi.org/10.21741/9781644902455-33

$$\beta^{(2+3)} \sim A_{(\omega_H \pm \omega_{L2})}, A_{(\omega_H \pm \omega_{L1})}, \ , \\ A_{(\omega_H \pm 2\omega_{L2})}, A_{(\omega_H \pm \omega_{L2} \pm \omega_{L2})}, A_{(\omega_H \pm 2\omega_{L2} \pm \omega_{L2})} \ and \ A_{(\omega_H \pm 2\omega_{L2} \pm \omega_{L2})}. \quad (7)$$

where the superscript (2+3) of β indicates the nonlinear parameter considering the second and third displacement field u_2 and u_3. From the solution of u_2 and u_3, all sidebands components are related to A_H and A_{L2}. Hence, the nonlinear parameters of AMVA technique can be defined as

$$\beta^{(2)} \ and \ \beta^{(2+3)} \sim \frac{\sum A_s}{A_H A_{L2}}. \quad (8)$$

where A_s is the amplitude of sideband components.

Experiment

The PRGs were produced by the First Graphene Ltd in Perth, WA, Australia, and the particle size is 43 μm. Ordinary Portland cement (OPC) was provided by Adelaide Brighton Cement LTD following Australian Standard AS 3972-2010 [13]. The fine coarse was nature sands with 2.36 mm maximum particle size. In addition, MasterGlenium SKY 8100 complying with Australian Standard AS 1478.1-2000 was the superplasticizer. The designed mix of PRG mortars used the optimized PRG dosage in previous studies [2, 3], which investigated the improvement of mechanical strength of PRG cement-based material. The details are listed in Table 1. There were three specimens of this batch in the size of $40mm \times 40mm \times 180mm$, namely S1, S2, and S3. These PRG mortar specimens were tested by the AMVA technique and UPV technique at the intact state. Afterward, thermal damages were induced into these specimens. Specimen S1 was heated to 100℃ while the target temperature of S2 and S3 were 250℃ and 360℃, respectively.

Table 1. *Designed mixed of PRG mortar specimens*

PRG [%]	PRG size [μm][14]	Cement [kg/m^3]	Water [kg/m^3]	Sand [kg/m^3]	Superplasticizer [kg/m^3]
0.07	43	527	255.6	1448	1.4

* The percentage of PRG is based on the weight of cement binder.

The schematic set-up of AMVA technique is presented in Fig.1. A pre-modulated LF pump wave $A_{L2}\cos(\omega_{L2}\tau + \phi_{L2})[1 + A_{L1}\cos(\omega_{L1}\tau + \phi_{L1})]$ was input into the signal generator and then fed by a power amplifier. The electromagnetic shaker was used to emit the LF pump wave with the help of a design clamp which was used to provide connection between the specimen and shaker firmly. In addition, a continuous HF probe wave $A_H\cos(\omega_H\tau + \phi_H)$ was generated by the functional generator, transmitted into the signal amplifier and then emitted by a transducer. The LF pump wave and HF probe wave propagated through the PFG mortar specimen and were received by another transducer. The receiving signal was obtained by the digitizer for further analysis. Furthermore, the UPV tests were conducted following ASTM C597-09 [14].

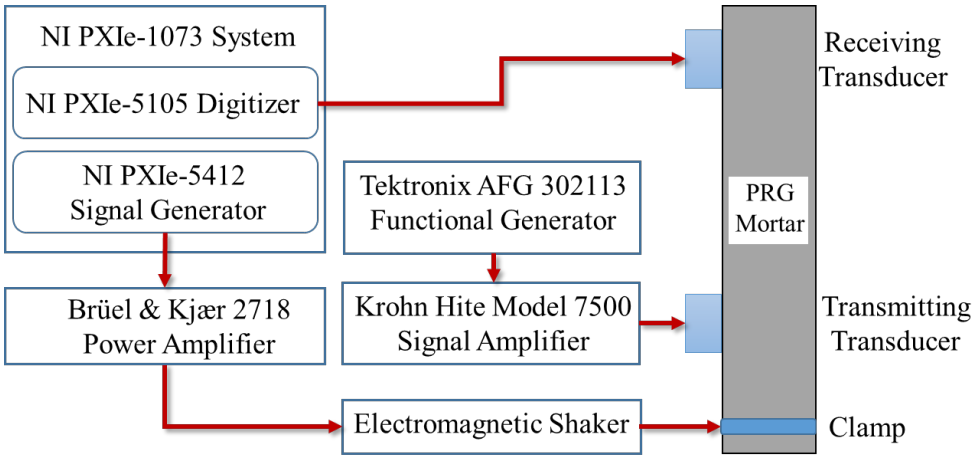

Fig. 1 Schematic set-up of AMVA technique

Results and discussions

The receiving signals of AMVA technique were processed by fast Fourier transform (FFT) into frequency domain as shown in Fig.2. It can be seen that, at the intact state, there are still some sidebands generated, which indicates that the PRG mortar specimens have some inherent defects even at the intact state. In general, these defects are the weakened parts of the structures that develop and combine with other damages to form macro-scale damages to threaten the safety of structures. Hence, these inherent defects should be noted and monitored. After the thermal treatment, the number and magnitude of the sidebands increase. It was found that in the PFG specimen after exposure to the high temperature, the sidebands corresponding to $(\omega_H \pm \omega_{L2}), (\omega_H \pm \omega_{L1}), (\omega_H \pm 2\omega_{L2}), (\omega_H \pm \omega_{L2} \pm \omega_{L2}), (\omega_H \pm 2\omega_{L2} \pm \omega_{L2})$ and $(\omega_H \pm 2\omega_{L2} \pm \omega_{L2})$ all showed in the frequency domain, instead of only $(\omega_H \pm \omega_{L2})$ and $(\omega_H \pm \omega_{L2} \pm \omega_{L2})$ derived from $\beta^{(2)}$. Therefore, it is meaningful to consider higher order effects to evaluate damages using AMVA techniques.

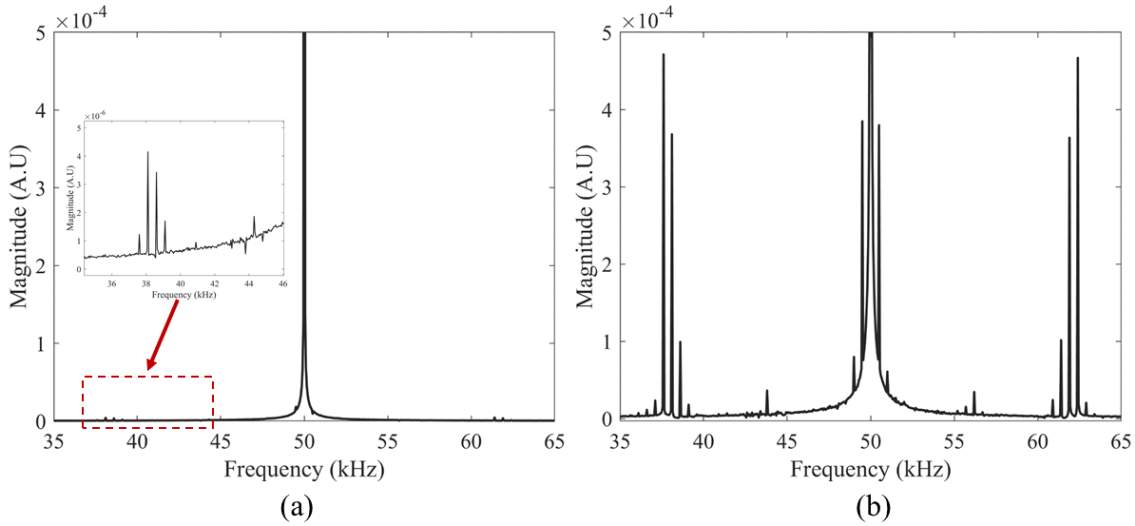

Fig. 2 Frequency domain: (a) intact state, (b) after thermal treatment

All nonlinear parameters of $\beta^{(2)}$ and $\beta^{(2+3)}$ were transferred into dimensionless indexes for better comparison. It can be seen that with more intensive thermal treatments, all the dimensionless indexes increased sharply. However, the tendency of dimensionless index of wave velocity c is quite gentle. These results demonstrate that the nonlinear measurements are significantly sensitive compared with the wave velocity. Nevertheless, the tendency of $\beta^{(2)}$ and $\beta^{(2+3)}$ were similar, the

results considering higher-order effects are more consistent with the phenomena seen in the experiments.

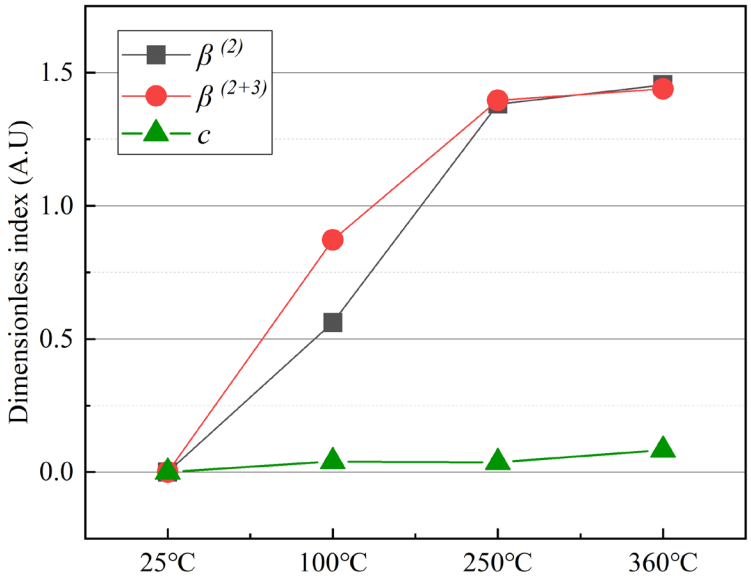

Fig. 3 Dimensionless index of $\beta^{(2)}$,$\beta^{(2+3)}$ and c

Conclusion

In this study, a new AMVA technique for assessing thermal damage in PRG mortar is proposed. In addition, a nonlinear parameter is established using a new third-order solution for an amplitude-modulated low-frequency pump wave and a high-frequency probe wave propagating in an infinite isotropic material. The experimental results demonstrate that the nonlinear parameter of AMVA technique can characterize the different levels of thermal damage in PRG material, and it is much one to two orders larger than the linear measurements of UPV test. In conclusion, the proposed AMVA technique is a potential tool to detect and monitor thermal damage in cement-based structures.

Reference

[1] Ho, V.D., et al., *Enhancing the performance and environmental impact of alkali-activated binder-based composites containing graphene oxide and industrial by-products.* Construction and Building Materials, 2021. **284**: p. 122811. https://doi.org/10.1016/j.conbuildmat.2021.122811

[2] Ho, V.D., et al., *Influence of pristine graphene particle sizes on physicochemical, microstructural and mechanical properties of Portland cement mortars.* Construction and Building Materials, 2020. **264**: p. 120188. https://doi.org/10.1016/j.conbuildmat.2020.120188

[3] Ho, V.D., et al., *Investigating the reinforcing mechanism and optimized dosage of pristine graphene for enhancing mechanical strengths of cementitious composites.* RSC Advances, 2020. **10**(70): p. 42777-42789. https://doi.org/10.1039/D0RA07639B

[4] Sohn, H., et al., *Nonlinear ultrasonic wave modulation for online fatigue crack detection.* Journal of Sound and Vibration, 2014. **333**(5): p. 1473-1484. https://doi.org/10.1016/j.jsv.2013.10.032

[5] Klepka, A., et al., *Structural damage detection based on nonlinear acoustics: application examples*, in *Nonlinear Ultrasonic and Vibro-Acoustical Techniques for Nondestructive Evaluation*. 2019, Springer. p. 139-174. https://doi.org/10.1007/978-3-319-94476-0_4

[6] Chen, J., et al., *Characterization of concentrated and distributed cracks in concrete using a harmonic wave modulation technique.* Materials and Structures, 2018. **51**(1): p. 1-10. https://doi.org/10.1617/s11527-017-1129-0

[7] Chen, J., J. Ren, and T. Yin, *Nondestructive evaluation of notched cracks in mortars by nonlinear ultrasonic technique.* Nondestructive Testing and Evaluation, 2016. **31**(2): p. 109-121. https://doi.org/10.1080/10589759.2015.1078331

[8] Duffour, P., M. Morbidini, and P. Cawley, *A study of the vibro-acoustic modulation technique for the detection of cracks in metals.* The Journal of the Acoustical Society of America, 2006. **119**(3): p. 1463-1475. https://doi.org/10.1121/1.2161429

[9] Frouin, J., et al. *In-situ monitoring of acoustic linear and nonlinear behavior of titanium alloys during cycling loading*. in *Nondestructive Evaluation of Aging Materials and Composites III*. 1999. SPIE. https://doi.org/10.1117/12.339838

[10] Dziedziech, K., et al., *Efficient swept sine chirp excitation in the non-linear vibro-acoustic wave modulation technique used for damage detection.* Structural Health Monitoring, 2018. **17**(3): p. 565-576. https://doi.org/10.1177/1475921717704638

[11] Yin, T., et al., *Amplitude-Modulation Vibro-Acoustic Technique for Damage Evaluation.* Structural Health Monitoring, 2022: p. 14759217221106209. https://doi.org/10.1177/14759217221106209

[12] Yin, T., C.-T. Ng, and A. Kotousov, *Damage detection of ultra-high-performance fibre-reinforced concrete using a harmonic wave modulation technique.* Construction and Building Materials, 2021. **313**: p. 125306. https://doi.org/10.1016/j.conbuildmat.2021.125306

[13] *Australian Standard, in General purpose and blended cements*. 2010, Standards Australia International Ltd: Sydney, NSW 2001, Australia.

[14] International, A., *ASTM C597-09 Standard Test Method for Pulse Velocity Through Concrete*. 2009.